



**HAL**  
open science

## Elastic properties of tensile nitrogen-plasma-treated multilayer silicon nitride films

M. Braccini, F. Volpi, Arnaud Devos, G. Raymond, D. Benoit, Pascal Morin

► **To cite this version:**

M. Braccini, F. Volpi, Arnaud Devos, G. Raymond, D. Benoit, et al.. Elastic properties of tensile nitrogen-plasma-treated multilayer silicon nitride films. *Thin Solid Films*, 2014, 551, pp.120-126. 10.1016/j.tsf.2013.11.012 . hal-00925380

**HAL Id: hal-00925380**

**<https://hal.science/hal-00925380>**

Submitted on 30 Jun 2023

**HAL** is a multi-disciplinary open access archive for the deposit and dissemination of scientific research documents, whether they are published or not. The documents may come from teaching and research institutions in France or abroad, or from public or private research centers.

L'archive ouverte pluridisciplinaire **HAL**, est destinée au dépôt et à la diffusion de documents scientifiques de niveau recherche, publiés ou non, émanant des établissements d'enseignement et de recherche français ou étrangers, des laboratoires publics ou privés.

1 **Elastic properties of tensile nitrogen-plasma-treated multilayer silicon nitride films**

2

3 M. Braccini<sup>a\*</sup>, F. Volpi<sup>a</sup>, A. Devos<sup>b</sup>, G. Raymond<sup>a,c</sup>, D. Benoit<sup>c</sup>, P. Morin<sup>c,d</sup>

4 <sup>a</sup> SIMaP Grenoble-INP/CNRS/UJF – BP75 – 38402 St Martin d'Hères cedex – France

5 <sup>b</sup> IEMN – UMR8250 CNRS – avenue Poincaré BP 69 – 59652 Villeneuve d'Ascq cedex -  
6 France

7 <sup>c</sup> STMicroelectronics – 850 rue Jean Monnet – 38926 Crolles cedex – France

8 <sup>d</sup> STMicroelectronics - Nanotech Center - 257 Fuller road - 12208 Albany NY - USA

9

10

11 **Abstract**

12 Highly stressed silicon nitride thin films are used in gate first complementary metal oxide  
13 semiconductors to improve mobility in the silicon channel. Compressive stresses improve  
14 hole mobility in p-type MOS transistors while tensile stresses increase electron mobility in n-  
15 type MOS devices. High levels of compressive stress are easily reached in plasma enhanced  
16 chemical vapor deposited films by using the plasma power setting at a temperature compatible  
17 with the integration flow. Tensile stresses are more difficult to obtain with a plasma process  
18 because of the low temperatures required. Nevertheless, some post-treatments have been  
19 developed based on desorption of hydrogen that has been incorporated during the deposition  
20 step. The present study concerns one of those treatments consisting in a sequential deposition  
21 / nitrogen plasma treatment of elementary layers. Both nano-indentation and picosecond  
22 ultrasonic methods are used to measure the Young's modulus of the obtained silicon nitride  
23 thin films. The effect of the plasma treatment on the change in elastic modulus is investigated

---

\* Corresponding author: [mauriel.braccini@simap.grenoble-inp.fr](mailto:mauriel.braccini@simap.grenoble-inp.fr), tel +33.476.826.539, fax +33.476.826.677, SIMaP – BP75- F-38402 Saint Martine d'Hères cedex - France

1 through the relationship with other properties like mass density and the concentration of Si-N  
2 bonds.

3

4 **Keywords:** PECVD silicon nitride; thin film; Young's modulus; nitrogen plasma treatment;  
5 picosecond ultrasonics.

6

## 7 **1. Introduction**

8 In several applications, residual stress in thin films should be avoided, but in complementary  
9 metal oxide semiconductor (CMOS) applications it can be beneficial. Indeed, mechanical  
10 strain in the silicon channel is a way to increase carrier mobility [1,2]. This can be performed  
11 by the use of a highly stressed film. Silicon nitride is one of the most frequently used  
12 materials for this purpose in the CMOS process [3,4]. Stresses are then introduced in the  
13 silicon nitride film which is used as the **Contact-Etch-Stop Layer (CESL)** in standard  
14 integration flows. The dual stress liner combines a compressive film above p-type MOS  
15 transistors to improve hole mobility and a tensile film above n-type MOS transistors to  
16 increase electron mobility.

17 Plasma-enhanced chemical vapor deposition (PECVD) is widely used for the CESL silicon  
18 nitride film process because it allows for low temperature deposition which minimizes the  
19 impact on devices ( $<400^{\circ}\text{C}$ ). Moreover, PECVD allows for the added possibility of tuning the  
20 stress through the plasma power setting. Compressive stresses are obtained by increasing  
21 plasma power. This leads to ion bombardment of the growing film surface and the  
22 incorporation of hydrogen. High levels of tensile stress are more difficult to obtain. As a  
23 consequence of low temperatures required for the CESL application, sufficient plasma power  
24 is needed to allow the chemical reaction to occur between the silicon precursor and ammonia.  
25 As a result, plasma power cannot be tuned to low levels and tensile stress is not favored

1 during the deposition stage. Nevertheless, some works have been done on post-treatment  
2 processes and it has been demonstrated that partial removal of hydrogen after deposition  
3 increases residual stress toward higher tensile values [5,6]. Thermal treatment on PECVD  
4 films leads to an increase of the stress correlated to hydrogen desorption [7]. This hydrogen  
5 loss results from the generation of Si-N bonds through hydrogen dissociation [7]. The  
6 network of Si-N bonds then densifies and tensile stresses develop. Some similar effects are  
7 obtained with other post-treatments like UV cure process or sequential nitrogen plasma  
8 treatment.

9 During the de-hydrogenation post-treatments of PECVD silicon nitride films, the  
10 densification of the Si-N bond network can also lead to changes in the elastic properties.  
11 Indeed, in bulk materials as well as in thin films, the elastic modulus depends on the mass  
12 density. In particular, Wamsley et al. [8] studied the influence of deposition temperature on  
13 the properties of PECVD silicon nitride thin film. They demonstrated a strong correlation  
14 between Young's modulus and density in those films. Secondly, in SiO<sub>2</sub> dielectric amorphous  
15 material, a correlation has been shown between Young's modulus and the Si-O-Si bond  
16 concentration [9]. The same kind of correlation can be expected with the Si-N bond  
17 concentration in silicon nitride films. Finally, the elastic properties of silicon nitride films  
18 influence the transmission of strain to the silicon channel. It is interesting to investigate the  
19 change of those properties during post-treatments.

20 Nevertheless, measuring Young's modulus in very thin films is challenging. Many methods  
21 have been developed to determine Young's modulus in thin films. Among them, the nano-  
22 indentation method is probably the most used because it is easy to perform: no particular  
23 specimen preparation is needed. Only a low surface roughness is required, which is often the  
24 raw surface state of PECVD films. A typical nano-indentation experiment uses a hard  
25 diamond tip which is pressed into the surface of the specimen. Young's modulus and hardness

1 are determined from the load-displacement curve during tip penetration and unloading [10].  
2 But when performing nano-indentation experiment on a thin film the substrate properties  
3 contribute to the measurement [11]. Some other methods have been developed based on the  
4 free-standing layer such as the bulge test [12] or beam bending [13]. However, these tests  
5 require specimen fabrication that can be difficult if not impossible.

6 Mechanical properties can also be investigated using acoustic techniques. Surface Brillouin  
7 light scattering can reach the sound velocity of surface acoustic wave in the GHz range [14].  
8 The acoustic waves studied with this technique are those thermally excited in the sample. It  
9 can be very time-consuming to collect the photons scattered by such acoustic waves. Laser  
10 ultrasonic techniques are also frequently used to probe the elastic properties of micron and  
11 submicron films. In that case a laser excites some acoustic waves of various natures in the  
12 sample and another laser detects acoustic propagation through a measurement of the surface  
13 displacement. In Surface Acoustic Wave (SAW) Spectroscopy, a broadband SAW pulse is  
14 emitted and an interferometer measures the surface displacement at a distant place [15-16].  
15 For a thin single-layer on a substrate, the wave dispersion is affected by the substrate due to  
16 the fact that the acoustic wavelength is not short enough and a numerical modeling is  
17 required. The frequency range of the SAW technique (a few 100 MHz) limits its applicability  
18 to film thicker than 1 micron.  
19 Picosecond ultrasonics is also a laser technique but which focuses on longitudinal acoustic  
20 waves that propagate normally to the layers [17]. This technique can reach very high  
21 frequency (a few 100 GHz) and is thus suitable for probing very thin layers (down to 10 nm).  
22 The technique uses a pump-probe scheme to reach an ultimate time-resolution so that  
23 successive layers are immediately identified. In particular, there is no influence of the  
24 substrate.

1 Both nano-indentation and picosecond ultrasonic methods are used here to investigate elastic  
2 properties of PECVD silicon nitride thin films. The films are obtained by sequential  
3 deposition/nitrogen plasma treatment of elementary layers resulting in a particular film  
4 structure. The influence of the N<sub>2</sub> plasma treatment on the change in Young's modulus is  
5 studied in correlation with the evolution of other properties of the films like mass density and  
6 Si-N bond concentration. Deposition and post-treatment parameters are investigated such as  
7 the elementary layer thickness and the plasma treatment duration. Simple models are  
8 proposed to describe the influence of those two parameters on the Young's modulus.

9

## 10 **2. Experimental details**

### 11 2.1. Film deposition and treatment

12 The silicon-nitride films studied here are the same as in [18]. Those films are obtained by  
13 PECVD technique with short deposition steps alternating with pure nitrogen plasma treatment  
14 steps. The films were then formed by sequential deposition/plasma treatment steps and were  
15 finally composed of  $n$  elementary layers (see fig.1).

16 Two series of films were deposited. The first series of films have various elementary layer  
17 thicknesses, from 1.8 nm to 350 nm. The number of layers is optimized to obtain a total film  
18 thickness of about 350 nm. Two kinds of film in this series are: one without plasma treatment,  
19 and the other where each elementary layer was submitted to a 20 s nitrogen plasma treatment.

20 The second series of multilayer films have a constant layer thickness but the N<sub>2</sub>-plasma  
21 treatment duration has been varied from 0 to 80 s. The films are composed of 100 layers for a  
22 total thickness ranging from 320 to 350 nm depending on the plasma treatment duration, since  
23 layers tend to shrink during this treatment because of densification.

24

### 25 2.2. Physical and chemical characterizations

1 The films were characterized using some standard clean-room tool set including a FX100  
 2 spectroscopic ellipsometer, a Fourier Transform Infrared (FTIR) spectroscope (BIO RAD QS  
 3 2200A from Accent) and a high-precision weighting machine (Mentor SP3 from Metryx). A  
 4 specific analysis was performed to obtain an overall description of the films chemistry from  
 5 FTIR spectra [18]. This analysis is based on several approximations but it provides  
 6 quantitative bonds concentration results of  $10^{17}$  bonds.cm<sup>-2</sup> with an uncertainty of  $\pm 0.5.10^{17}$   
 7 bonds.cm<sup>-2</sup>.

8

### 9 2.3. Nano-indentation method

10 Nano-indentation technique is widely used in the study of thin films, to measure elastic  
 11 modulus and hardness. Nano-indentation measurements were performed on a MTS Nano  
 12 Instrument XP tool. We performed the measurements with a Berkovich indenter in a  
 13 Continuous Stiffness Measurement (CSM), according to the standard Oliver-Pharr protocol  
 14 [10]. Because our films are very thin (less than 400 nm) some substrate effects take place  
 15 [11]. Various models have been developed to take into account this effect [19-21]. We chose  
 16 the extrapolation method proposed by Perriot et al. [20]. This method is easy to implement  
 17 and adapted to the case where elastic modulus mismatch between film and substrate is low. In  
 18 this method, an empirical description is used to link the measured modulus  $E_{eq}^*$  to the reduced  
 19 elastic moduli of the film ( $E_f^* = E_f / (1 - \nu_f^2)$ ) and of the substrate ( $E_s^*$ ) according to the following  
 20 equation

$$21 \quad E_{eq}^* \left( \frac{a}{t} \right) = E_f^* + \frac{E_s^* - E_f^*}{1 + \left( x_o \frac{t}{a} \right)^n} \quad (1)$$

22 Where  $t$  is the film thickness and  $a$  the contact radius (see figure 2).  $x_o$  and  $n$  are two  
 23 adjustable parameters. For our calculations, since the ratio  $E_s^* / E_f^*$  varied between 1.2 and  
 24 1.7, we used values close to those obtained by Perriot et al. [20]:  $n = 1.27$  and  $x_o$  ranging

1 between 0.6 and 1.4. Figure 2 shows a typical fit obtained on measured nano-indentation  
2 modulus using this empirical relationship with  $E_s^* = 179$  GPa.

3

#### 4 2.4. Picosecond ultrasonic technique

5 One way to measure elastic properties in materials is to use acoustic wave propagation. In thin  
6 films this method is adapted using the picosecond ultrasonic technique [22]. In picosecond  
7 ultrasonics one implements a sonar-like technique at the submicron scale using an ultrafast  
8 laser in a pump-probe scheme. The strong optical absorption of a laser pulse (the pump) in the  
9 sample launches an ultra-short acoustic pulse. Thanks to another laser pulse (the probe),  
10 which is time delayed with respect to the pump, the propagation and reflections of the  
11 acoustic pulse are time-resolved (figure 3) [17,23-24]. In the case of a transparent sample, a  
12 thin metallic layer is deposited at the top acting as a transducer (15 nm of Aluminum here).  
13 By detecting acoustic echoes, one can reach the time-of-flight in the successive layers of the  
14 sample. From the thickness it is easy to deduce the longitudinal sound velocity. As sound  
15 velocities are related to elastic moduli, picosecond ultrasonics can be used for measuring  
16 mechanical properties of thin films. In isotropic material, the longitudinal sound velocity  $v_l$   
17 and the mass density  $\rho$  are related to the Young's modulus  $E$  and the Poisson's ratio  $\nu$   
18 according to [24]

$$19 \quad v_l = \sqrt{\frac{E(1-\nu)}{\rho(1+\nu)(1-2\nu)}} \quad (2)$$

20 The precision of this method depends highly on the precision in the measurement of the film  
21 thickness and its mass density. In our case, film thickness is measured from spectroscopic  
22 ellipsometry technique which rises to an error of 0.5%. Mass density is calculated from  
23 weighting the samples on a micro-balance leading to an error of about 1% due to the precision

1 of the instrument (0.01 mg) and the error on the film thickness. Finally, this leads to a  
2 precision of about 2% on the Young's modulus determination.

3 Picosecond ultrasonic experiments were carried on using a tunable Ti:Sapphire oscillator and  
4 a conventional pump and probe scheme at normal incidence. The laser produces 120 fs optical  
5 pulses at a repetition rate of 80 MHz. We used a pump centered at 800 nm and a 400 nm  
6 probe obtained by second harmonic generation in a  $\beta$ -BaB<sub>2</sub>O<sub>4</sub> crystal. That configuration  
7 offers a very convenient way of detecting the arrival of the acoustic pulse into the silicon  
8 substrate due to the strong acousto-optic response of silicon in the blue range [24]. Both  
9 beams are focused on the same point of the sample thanks to a 60 mm lens. The ratio between  
10 the pump and probe intensities is close to 1000:1. To improve the signal-to-noise ratio, the  
11 pump beam is chopped using an acousto-optic modulator and the output of the photodiode,  
12 which monitors the reflected probe, is amplified through a lock-in scheme. At  $t=0$ , the pump  
13 laser pulse is absorbed in the Al layer. The resulting thermal expansion generates a  
14 longitudinal acoustic pulse whose extension is fixed by the Al film thickness. Due to an  
15 acoustic mismatch between Al and SiN, a fast damped oscillation is detected close to zero. It  
16 is related to the part of the acoustic energy which is confined within the Al layer. The other  
17 part propagates towards the substrate and during propagation in the Si-N layer a low  
18 frequency is detected on the photo-elastic response [25]. Then the acoustic pulse enters the Si  
19 substrate and a strong and high frequency oscillation is detected (see the arrow in fig. 3. The  
20 time-delay at which such an oscillation starts exactly corresponds to the time-of-flight in the  
21 Si-N layer. The longitudinal sound velocity is deduced from the film thickness.

22

### 23 **3. Results**

24 For each specimen, the elastic modulus was measured by both the nano-indentation method  
25 and the picosecond ultrasonics. We can notice that these two techniques lead to similar

1 results, but with some difference that can reach up to 10 %. This difference can be attributed  
2 to various causes. The first one is the choice in Poisson's ratio. Indeed, in both methods two  
3 parameters are unknown; Young's modulus and Poisson's ratio. One often assumes a  
4 Poisson's ratio to estimate Young's modulus. So we try various values of Poisson's ratio for  
5 the silicon nitride thin films between 0.2 and 0.3 but none leads to a perfect match between  
6 picosecond ultrasonics and nano-indentation measurements. So the Poisson's ratio of the films  
7 was set to 0.23, which is the value for bulk silicon nitride. A second cause for the difference  
8 between nano-indentation and picosecond ultrasonics measurements stands in the substrate  
9 effect that disturb the nano-indentation measurements. Even if we combine CSM  
10 measurements with an extrapolation method to estimate the film modulus, our film  
11 thicknesses are in the limits of conventional nano-indentation ability. Then extrapolation is  
12 performed on a short range of data, particularly in the low indentation depth part ( $< 50$  nm)  
13 where the indenter tip defect effect takes place. For those reasons, the difference between the  
14 Young's moduli obtained from the two methods can be attributed to error in Young's modulus  
15 determination using nano-indentation on our films.

16 In figure 4, raw data from elastic modulus measurements are plotted according to two  
17 parameters: the elementary layer thickness  $e$  and the plasma treatment duration on each  
18 elementary layer. First, we can observe that whatever the elementary layer thickness, without  
19 plasma treatment the same value is obtained for the Young's modulus. This reference value is  
20  $103 \pm 5$  GPa (from picosecond ultrasonics,  $111 \pm 10$  GPa from nano-indentation). If the  
21 elementary layers are submitted to a 20 s plasma treatment, the elastic modulus becomes  
22 sensitive to their thickness. The Young's modulus seems to vary as a linear function of the  
23 inverse of the elementary layer thickness (see fig.4.a). In fig.4.b we can also observe an  
24 influence of the plasma treatment duration on the value of the Young's modulus of the film.  
25 For duration of 80 s, the Young's modulus increases from 103 GPa to 141 GPa, a 37%

1 increase. All those measured values are quite lower than the Young's modulus for bulk silicon  
2 nitride which is of the order of 300 GPa. We will see in the next section that this can be  
3 correlated to the mass density and to the structure of the films. Indeed, chemical and physical  
4 analyses were also performed on each sample and were presented in details in [18]. In  
5 particular, we can notice that the mass density in our films is lower than the one of full dense  
6 material. Moreover, similar evolutions were observed for film mass density according to  
7 elementary layer thickness and to plasma treatment duration. This evolution was linked to the  
8 chemical change induced by the plasma treatment on the elementary layers and the  
9 penetration depth of this treatment. In the next section we will demonstrate that Young's  
10 modulus evolution is also linked to the chemical change in the films and models previously  
11 developed in [18] will be extend to the elastic modulus.

12

#### 13 **4. Discussion**

14 In this section we aim to demonstrate relationships between elastic property of the films and  
15 their physical and chemical properties. During deposition, some hydrogen is trapped in the  
16 layer. N<sub>2</sub> plasma treatment leads then to some hydrogen dissociation and new Si-N bonds  
17 generation [18,26]. The chemical network is then strengthened, leading to higher density and  
18 higher stiffness. Nevertheless, Transmission Electronic Microscopy analysis of our films  
19 revealed that the plasma treatment affects only the top part of the elementary layers [18]. This  
20 can be related to a maximum penetration depth. This penetration depth can explain the  
21 influence of elementary layer thickness on the elastic modulus of the films with a 20 s  
22 treatment. Moreover, quantity of hydrogen dissociation, and so new Si-N bonds generation,  
23 depends on the treatment duration. But this is a chemical reaction with its own kinetics. So we  
24 can guess that the change in Young's modulus according to plasma treatment depends on this  
25 kinetic process.

1 From those two observations, simple models are proposed to describe the effect of elementary  
2 layer thickness and of plasma treatment duration on change in elastic modulus of the films.

3

#### 4 4.1. Layer thickness effect

5 Since the existence of a penetration depth has been evidenced by fine microstructure analysis,  
6 we can assume that there is a gradient of properties in the thickness of the elementary layers.

7 Let us consider, as a first approximation, that those layers are in fact bi-layers; at the bottom  
8 an untreated layer and at the top a treated layer, denser and stiffer.

9 The macroscopic density of such a bi-layer can be obtained by a simple rule of mixture:

$$10 \quad \rho_{eq} = \frac{e_t}{e} \rho_t + \frac{e_{ut}}{e} \rho_{ut} \quad (3)$$

11 Where the subscript  $t$  designates the treated part of the layer and  $ut$  the untreated one. The  
12 symbol  $\rho$  is used for mass density and  $e$  for thickness. Note that  $e_t + e_{ut} = e$ . Hence,  $\rho_{eq}$  is the  
13 macroscopic density of the system corresponding to the one measured on the film. From the  
14 measurement on untreated films we know the properties of the untreated part of the layer. If  
15 we assume that the thinner elementary layers of our study are completely treated by the N<sub>2</sub>  
16 plasma, we also know the density of the treated part. We can then deduce from our  
17 experimental data the penetration depth, or the thickness of the treated part of the layer. We  
18 find  $e_t = 2.25$  nm, which is indeed larger than the thinner elementary layers studied here (1.8  
19 nm). Of course, for layer thinner than this penetration depth the bi-layer model is reduced to  
20 one fully treated layer. This is why we have a saturation effect in the model for density in  
21 figure 6.b.

22 Dealing with the elastic modulus, the bi-layer model drives to more complex expressions. In  
23 the case of nano-indentation measurements for example, the indentation generates strain and  
24 stress both in the direction of indentation (ie normal to the layers plane) and in the plane of  
25 the layers. For those two loading directions of the bi-layer system there are two different rules

1 of mixture (fig. 5.a). One is called the parallel model and corresponds to a loading direction  
 2 parallel to the layers plane. It is described by an equation similar to (3):

$$3 \quad e \cdot E_{//} = e_t \cdot E_t + e_{ut} \cdot E_{ut} \quad (4)$$

4 The other one is called series model and described the equivalent elastic modulus when the  
 5 loading is perpendicularly to the plane of the layers:

$$6 \quad \frac{e}{E_{\perp}} = \frac{e_t}{E_t} + \frac{e_{ut}}{E_{ut}} \quad (5)$$

7 Those two models are plot in a Young's modulus versus  $1/e$  diagram in figure 5.b. using the  
 8 nano-indentation measurements on films with a 20 s plasma treatment. Here we assume that  
 9 the Poisson's ratio is not changed by the plasma treatment. We can notice that, except for a  
 10 particular point, the experimental data are bounded by the two models.

11 In the case of the picosecond ultrasonics method, we measure a time that corresponds to the  
 12 travel of a wave through the film. From this time-of-flight we deduce a sound velocity  
 13 according to the film thickness. And hence we calculate the Young's modulus thanks to an  
 14 equation where the mass density is needed. Even if the wave goes in the film in a direction  
 15 perpendicular to the layers plane, we cannot directly use equation (5). We have to use a bi-  
 16 layer approach to evaluate a mean sound velocity through the bi-layer system:

$$17 \quad v_l = \frac{e}{\Delta t} = \frac{(e_t + e_{ut})}{\Delta t_t + \Delta t_{ut}} \quad (6)$$

18 Where  $\Delta t_t$  and  $\Delta t_{ut}$  are the times needed by the sound to go through respectively the treated  
 19 layer and the untreated one. If we assume that the Poisson's ratio is not changed by the plasma  
 20 treatment, combining equations (2) and (6) leads to:

$$21 \quad \frac{e}{\sqrt{\frac{E_{eq}(1-\nu)}{\rho_{eq}(1+\nu)(1-2\nu)}}} = \frac{e_t}{\sqrt{\frac{E_t(1-\nu)}{\rho_t(1+\nu)(1-2\nu)}}} + \frac{e_{ut}}{\sqrt{\frac{E_{ut}(1-\nu)}{\rho_{ut}(1+\nu)(1-2\nu)}}} \quad (7)$$

1 Equation (7) looks like a series model but with an expression more complex than Eq.(5). In  
2 figure 6 we can observe a good agreement between this model and the experimental moduli  
3 measured by picosecond ultrasonic method.

4 So a simple first order model can be used to describe the effect of elementary layer thickness  
5 for short duration of N<sub>2</sub> plasma treatment. For longer treatment duration, we can observe in  
6 figure 4.b. a slow-down in the change of elastic modulus (after 40 s). This can be linked to a  
7 change in the densification mechanism. Indeed, for plasma treatment longer than 40 s, Si-N  
8 bond generation is still observed while hydrogen dissociation saturates [18]. So another  
9 mechanism becomes dominant in the Si-N bond generation process, probably some physical  
10 reorganization of the Si-N bonds network and/or porosity closure. We cannot identify clearly  
11 this mechanism but we can observe from the change in slope in figure 4.b. that its kinetics is  
12 slower than the kinetics of Si-N bond generation due to hydrogen dissociation. The next  
13 section is devoted to those kinetic aspects.

14

#### 15 4.2. Plasma treatment duration effect

16 Figure 7.a emphasizes the relationship between Young's modulus and Si-N bond  
17 concentration. Indeed, density and elastic modulus are intimately linked to the strength of the  
18 Si-N bond network. This relationship is similar to the one observed between mechanical  
19 properties and Si-O-Si bond network in low-*k* materials [9] for example. Let us consider the  
20 relative evolution of one of the film property as

$$21 \quad \Delta P = \frac{P(t) - P^0}{P^\infty - P^0} \quad (8)$$

22 Where  $P(t)$  is the considered property after a plasma treatment duration of  $t$ , and  $P^0$  and  $P^\infty$   
23 are respectively the initial value of this property, before any plasma treatment, and its final  
24 value, after an infinite time of treatment. We can notice that the relative evolution of the  
25 Young's modulus, the mass density and the Si-N bond concentration follow the same kinetics

1 (see figure 7.b). This evolution is different from the one of the internal stress that saturates  
2 after about 20 seconds of treatment time.

3 In agreement with the previous discussion, the Si-N bond generation results from two  
4 mechanisms that dominate the process successively. Then the reaction kinetics happens in two  
5 stages, the second one being slower.

6 Even if this second mechanism is not clearly identified, as a first approximation, we can  
7 assume that its kinetics is similar to the Si-N bond generation due to hydrogen dissociation:

$$8 \quad \frac{d[SiN]_i}{dt} = -k_i^n \left( [SiN] - [SiN]_i^\infty \right)^n \quad (9)$$

9 Where  $n$  is the order of the reaction. The subscript  $i$  indicates the Si-N bond generation  
10 mechanism and is equal to 1 or 2. Hence  $k_i^n$  and  $[SiN]_i^\infty$  are respectively the  $n$ -order reaction  
11 rate and the final concentration after infinite plasma treatment for mechanism  $i$ . If we consider  
12 first-order reaction kinetics ( $n=1$ ), the integration of equation (9) leads to

$$13 \quad [SiN](t) = \left( [SiN]^0 - [SiN]_i^\infty \right) \exp(-k_i t) + [SiN]_i^\infty \quad (10)$$

14 Where  $[SiN]_i^0$  is the initial concentration of Si-N bonds in the film.

15 Considering a mechanism change after 20 seconds of treatment, a regression method is used  
16 to obtain  $k_1$  and  $[SiN]_1^\infty$  for short times and  $k_2$  and  $[SiN]_2^\infty$  for long times. After optimization of  
17 those model parameters a good agreement is obtained with the experimental measurements of  
18 Si-N bond concentration (fig.8.a). So, even if our kinetics model is not rigorous physically  
19 speaking, it is sufficient in describing our data and taking into account the change in reaction  
20 kinetics.

21 According to the correlation between elastic modulus and Si-N bond concentration, we expect  
22 the same kinetics behavior in the Young's modulus change during plasma treatment. So we  
23 use the same model to describe this change, with the same reaction rates. After optimization  
24 of the infinite value of elastic modulus for each kinetics stage we obtain a good agreement

1 between our simple model and the experimental measurements from the picosecond ultrasonic  
2 method (fig.8.b):

$$3 \quad \Delta E = E(t) - E^0 = (E_i^\infty - E^0) [1 - \exp(-k_i t)] \quad (11)$$

4 The optimized parameters for the model are: for stage 1,  $k_1 = 0.157 \text{ s}^{-1}$  and  $E_1^\infty = 129 \text{ GPa}$ ; for  
5 stage 2,  $k_2 = 0.042 \text{ s}^{-1}$  and  $E_2^\infty = 141 \text{ GPa}$ . Those results are in agreement with our previous  
6 work on the effect of  $\text{N}_2$  plasma treatment on the internal stress evolution. Indeed, the interest  
7 in the sequential  $\text{N}_2$  plasma treated silicon nitride films studied here is the development of  
8 high tensile internal stress. So in our previous work the stress change in the films was  
9 specifically investigated [18]. This previous work drives to the conclusion that the stress  
10 change is more sensitive to the first mechanism responsible of the Si-N bond generation,  
11 which is the hydrogen dissociation. This is in agreement with other work on nitride films [7].  
12 So when this mechanism is no longer dominant, the stress development in the films saturates  
13 (figure 7.b). This is why the stress change kinetics is described by an equation similar to  
14 equations (10) and (11) but with only one stage and a rate equal to  $k_1$ .

15

## 16 **5. Conclusions**

17 The elastic properties of PECVD silicon nitride films were studied. The films were processed  
18 by sequential deposition and nitrogen plasma treatment in order to obtain high tensile stress.  
19 Consequently, those films have a specific structure consisting of  $n$  elementary layers. The  
20 effects of elementary layer thickness and plasma treatment duration on Young's modulus were  
21 investigated. In particular, a picosecond ultrasonics method gave accurate measurements on  
22 the change in elastic modulus in the films due to the plasma treatment.  
23 Thus, it was demonstrated that the elementary layer thickness has an influence on the elastic  
24 modulus of the film if some plasma treatment is realized. This effect is due to a maximum

1 penetration depth of the plasma in the elementary layers and can be modeled by a bi-layer  
2 approach.  
3 A change of the Young's modulus with the plasma treatment duration was also observed. This  
4 change can be related to the generation of Si-N bonds during the treatment. Indeed, during  
5 nitrogen plasma treatment of the PECVD films, Si-N bond concentration increases inducing a  
6 strengthening of the Si-N network and resulting in an increase of both the mass density and  
7 Young's modulus. Nevertheless, different mechanisms seem to contribute to the Si-N bond  
8 generation. For short time treatment, the dominating mechanism is hydrogen dissociation. But  
9 for longer times ( $> 40s$ ) this mechanism saturates and some other mechanisms contribute to  
10 the Si-N bond generation. At this point, those mechanisms cannot be clearly identified, but  
11 they lead to a slower kinetics of bond generation. Thus, a two staged reaction model was  
12 proposed to describe the modulus change kinetics. This simple model, based on first order  
13 reaction kinetics, is in good agreement with the Young's modulus measurements.

14

## 15 **References**

- 16 [1] K. Rim, K. Chan, L. Shi, Boyd , Electron Devices Meeting, San Francisco, USA, 8-10  
17 December, 2003, IEDM Technical Digest. IEEE International (2003) 49.
- 18 [2] S.E. Thompson, G. Sun, Y.S. Choi, T. Nishida, IEEE Trans. Elec. Dev. 53 (2006) 1010.
- 19 [3] S. Ito, H. Namba, K. Yamaguchi, T. Hirata, Electron Devices Meeting, San Francisco,  
20 USA, December 10-13, 2000 IEDM Technical Digest. IEEE International (2000) 247.
- 21 [4] F. Boeuf, F. Arnaud, M.T. Basso, D. Sotta, Electron Devices Meeting, San Francisco,  
22 USA, December 13-15, 2004 IEDM Technical Digest. IEEE International (2004) 425.
- 23 [5] J. Thurn, R. F. Cook, M. Kamarajugadda, L. C. Stearns, Thin Films: Stresses and  
24 Mechanical Properties IX, Boston, USA, 26-29 November, 2001, Mater. Res. Soc. Symp.  
25 Proc. 695 (2001) L3.9.1.

- 1 [6] P.J. Hughey, R.F.Cook, Thin Solid Films 460 (2004) 7.
- 2 [7] P.J. Hughey, R.F. Cook, J. Appl. Phys. 97 (2005) 114914.
- 3 [8] B.A Wamsley., Y. Liu, X.Z. Hu, M.B. Bush, K.J. Winchester, M. Martyniuk, J.M. Dell, L.
- 4 Faraone, J. Appl. Phys. 98 (2005) 044904.
- 5 [9] V. Jousseume, C. Le Cornec, F. Ciaramella, L. Favennec, A. Zenasni, G. Simon, J.P.
- 6 Simon, G. Gerbaud, G. Passemard, Materials, Technology and Reliability of Low-k
- 7 Dielectrics and Copper Interconnects, San Francisco, USA, 17-21 April, 2006, Mater. Res.
- 8 Soc. Symp. Proc. 914 (2006) F04.
- 9 [10] W.C. Oliver, G.M. Pharr, J. Mater. Res. 7 (1992) 1564.
- 10 [11] R. Saha, W.D. Nix, Acta mater. 50 (2002) 23.
- 11 [12] M.K. Small, W.D. Nix, J. Mater. Res. 7 (1992) 1553.
- 12 [13] J.-A. Schweitz, J. Micromech. Microeng. 1 (1991) 10.
- 13 [14] P. Zinin, M. H. Manghnani, X. Zhang, H. Feldermann, C. Ronning, H. Hofsäss, J. Appl.
- 14 Phys. 91 (2002) 4196.
- 15 [15] A G Every, Meas. Sci. Technol. 13 (2002) R21.
- 16 [16] Y.-C. Shena, P. Hess, J. Appl. Phys. 82 (1997) 4758.
- 17 [17] C. Thomsen, H. T. Grahn, H. J. Maris, J. Tauc, Phys. Rev. B 34 (1986) 4129.
- 18 [18] P. Morin, G. Raymond, D. Benoit, D. Guiheux, R Pantel., F. Volpi, M Braccini., J. Vac.
- 19 Sci. Technol. A29 (2011) 041513.
- 20 [19] J Mencik., D. Munz, E. Quandt, E.R. Weppelmann, M.V. Swain, J. Mater. Res. 12
- 21 (1997) 2475.
- 22 [20] A. Perriot, E Barthel., J. Mater. Res. 19 (2004) 600.
- 23 [21] H. Li, J.J. Vlassak, J. Mater. Res. 24 (2009) 1114.
- 24 [22] H.T. Grahn, H.J. Maris, J. Tauc, IEEE Journal of Quantum Physics 25 (1989) 2562.

- 1 [23] B. Bonello, B. Perrin, E. Romatet, J.C. Jeannet, *Ultrasonics* 35 (1997) 223.
- 2 [24] P.A. Mante, J.F. Robillard, A. Devos, *Appl. Phys. Lett.* 93 (2008) 071909.
- 3 [24] A. Devos, R. Cote, *Phys. Rev. B* 70(12) (2004) 125208.
- 4 [25] A. Devos, R. Cote, G. Caruyer, A. Lefebvre, *Appl. Phys. Lett.* 86 (2005) 211903.
- 5 [26] Y. Saito, T. Kagitama, S. Nakajima, *Jpn. J. Appl. Phys.* 42 (2003) L1175.
- 6

1 **Figure captions**

2 Fig.1 . Multilayer film structure as obtained after sequential deposition/plasma treatment  
3 technique (Transmission Electronic Microscope using bright field filter).

4

5 Fig. 2. Reduced modulus obtained by CSM nano-indentation method as a function of relative  
6 penetration. Dashed line corresponds to the Perriot et al. model [20].

7

8 Fig. 3. Schematic view of the picosecond ultrasonic setup and experimental signal obtained on  
9 a SiN/Si sample. Close to 35 ps a high frequency burst is detected as the acoustic pulse  
10 penetrates the Si substrate (see the arrow). That delay corresponds to the acoustic time-of-  
11 flight in the SiN layer.

12

13 Fig. 4. Young modulus evolution according to (a) the elementary film thickness, (b) the  
14 plasma treatment duration. (squares: nano-indentation; triangles: picosecond ultrasonics).

15

16 Fig.5.: Bi-layer modeling of the elastic modulus measured by nano-indentation: (a)  
17 schematics of the parallel and series models; (b) comparison with the experimental data.

18

19 Fig. 6. Bi-layer modeling of the density and of the elastic modulus measured by picosecond  
20 ultrasonic method.

21

22 Fig. 7. (a) Young's modulus as a function of Si-N bonds concentration; (b) Internal stress,  
23 Young's modulus, density and Si-N bonds generation change during plasma treatment.

24

- 1 Fig. 8. Comparison of the kinetics model (a) with Si-N bonds generation and (b) with the
- 2 Young's modulus change during plasma treatment

Figure 1

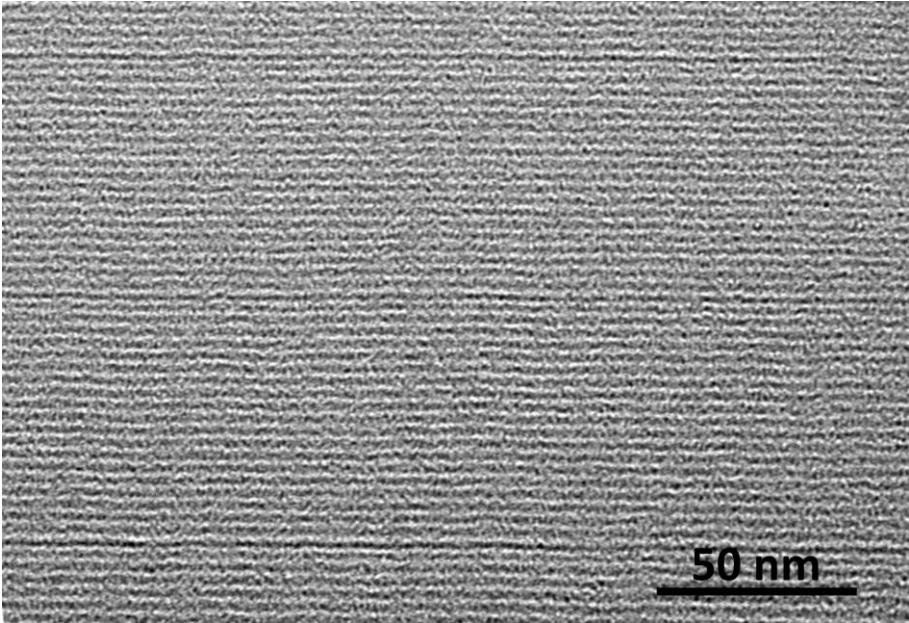


Figure 2

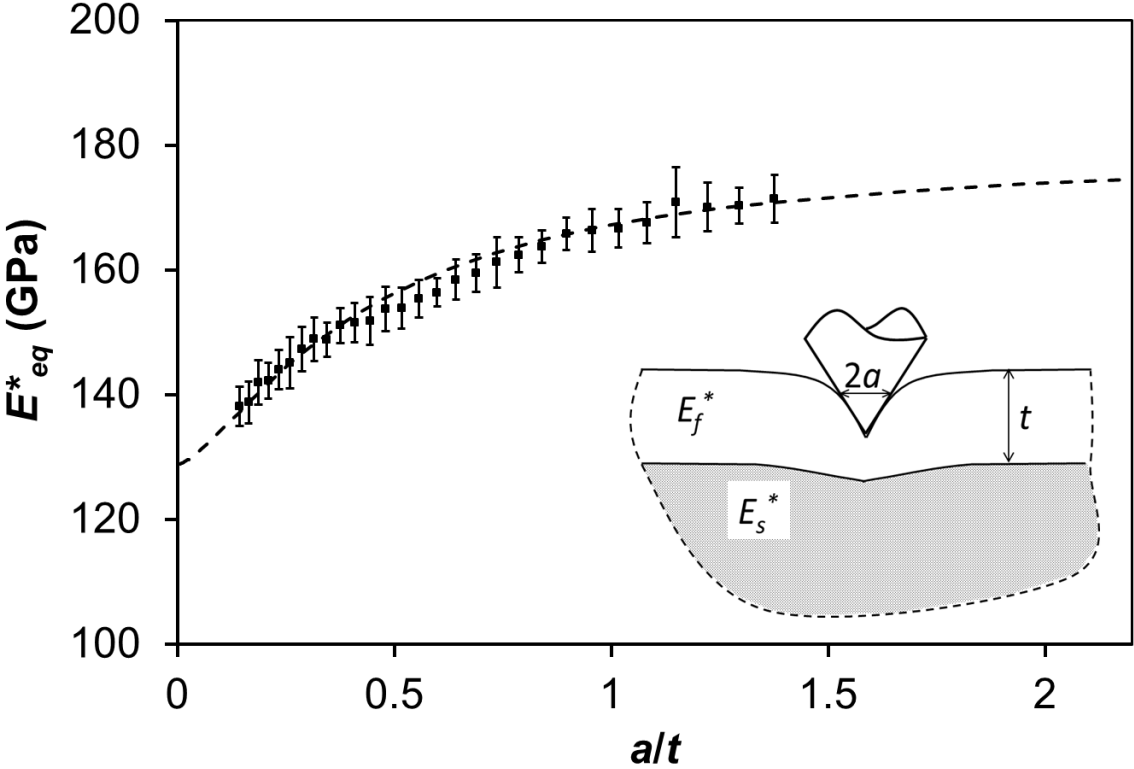


Figure 3

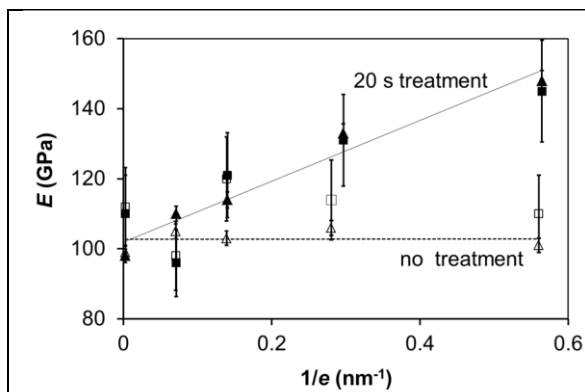
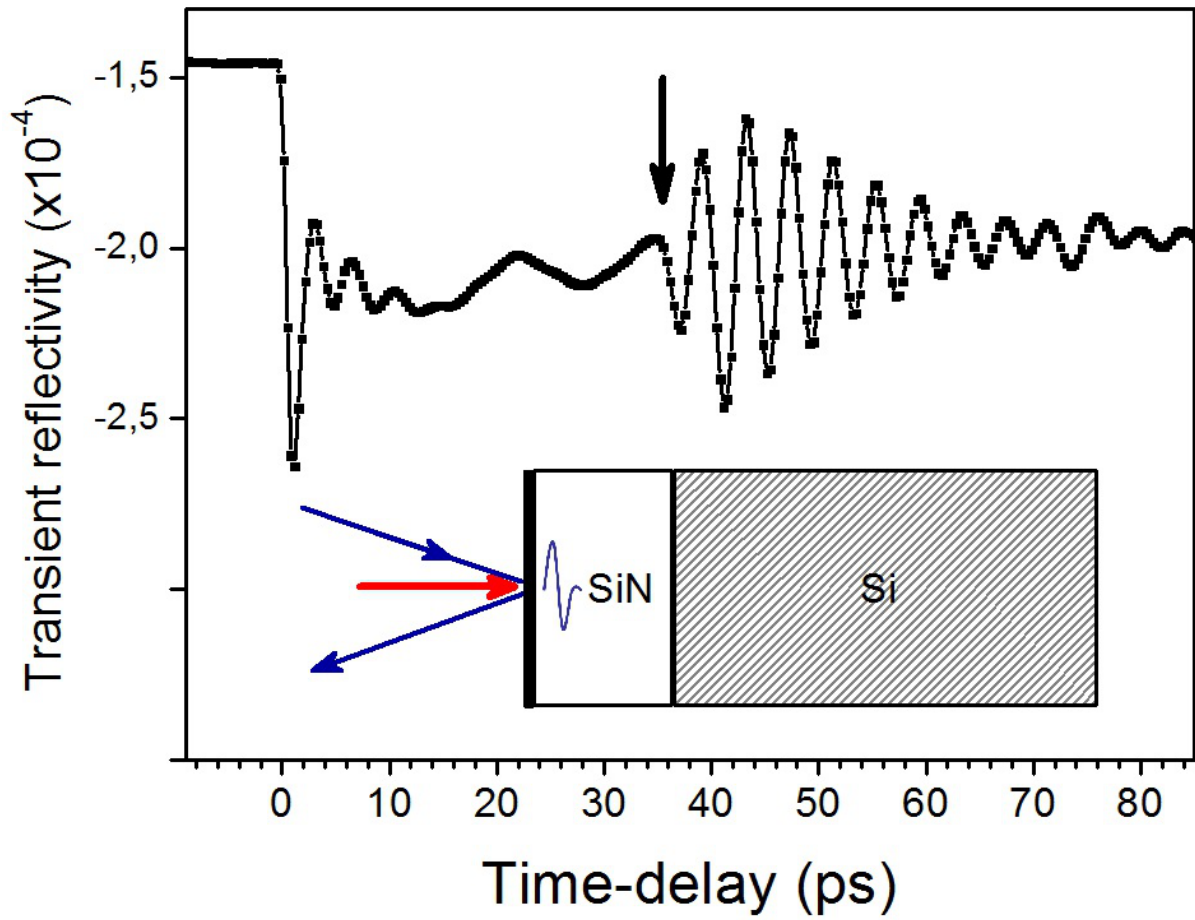


Figure 4.a.

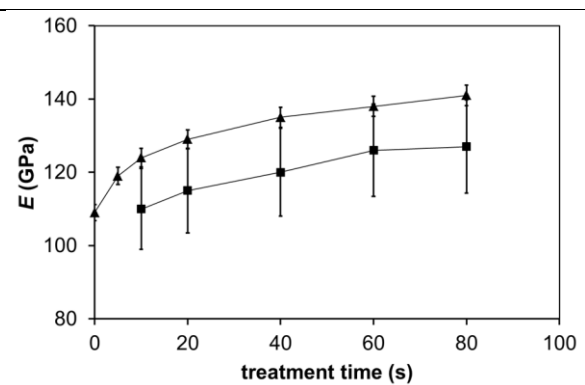


Figure 4.b.

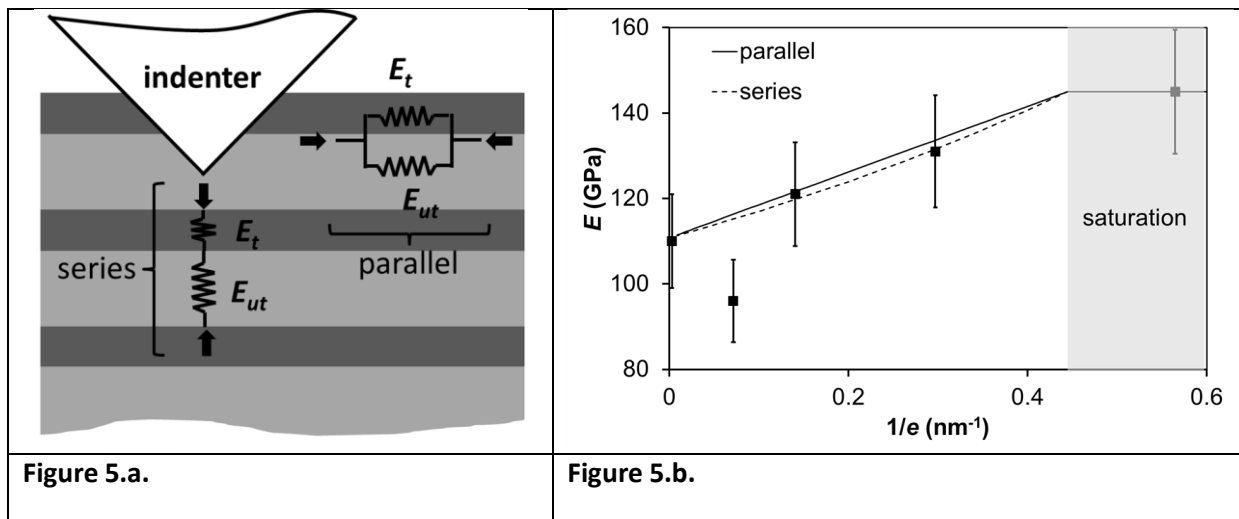
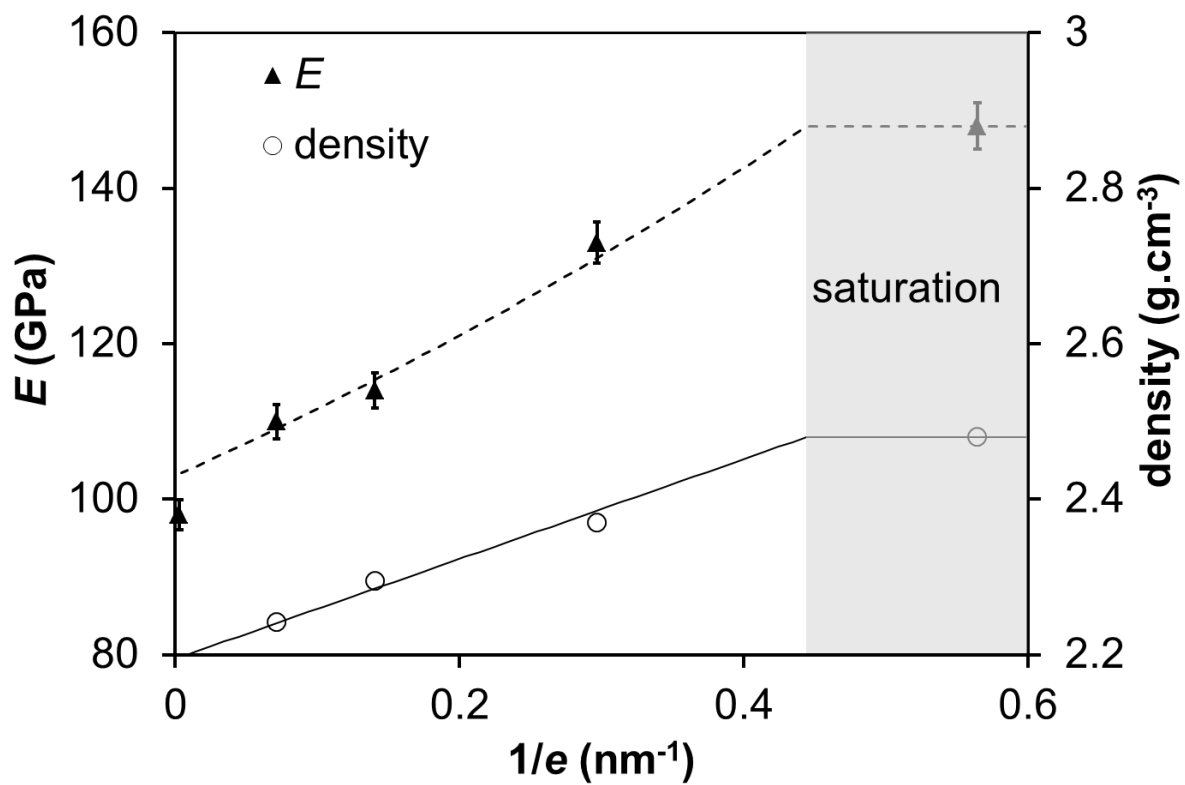


Figure 6



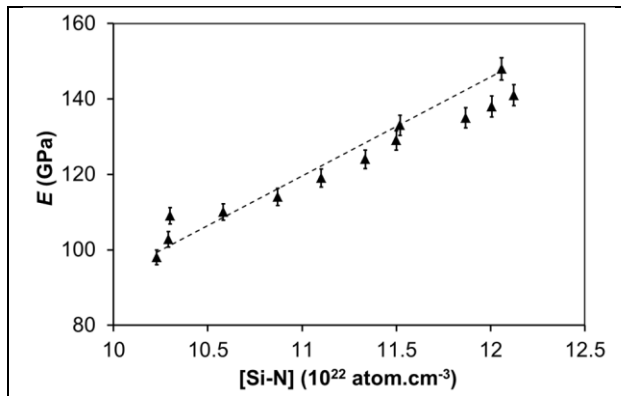


Figure 7.a.

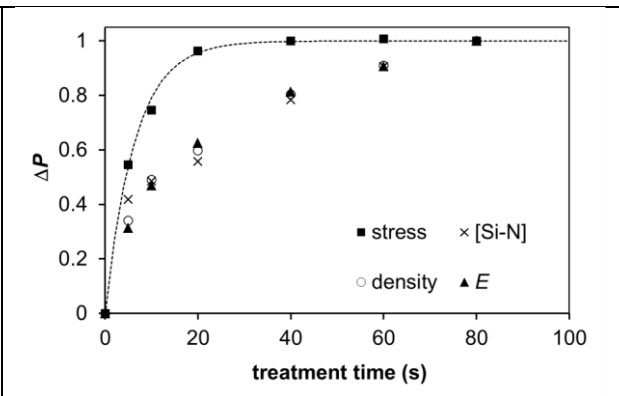


Figure 7.b.

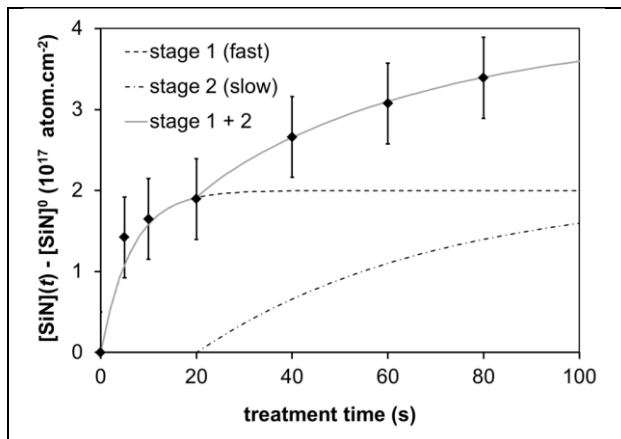


Figure 8.a.

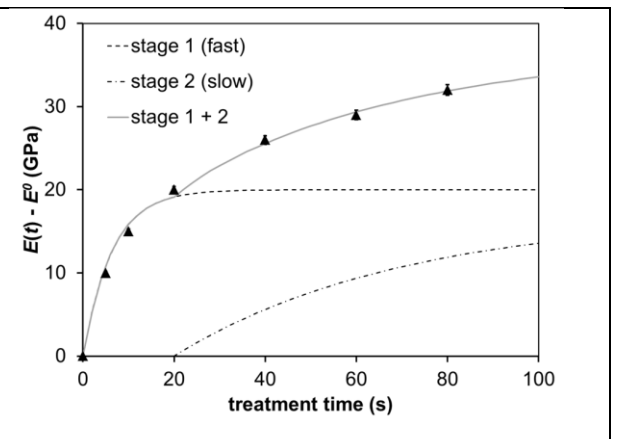


Figure 8.b.